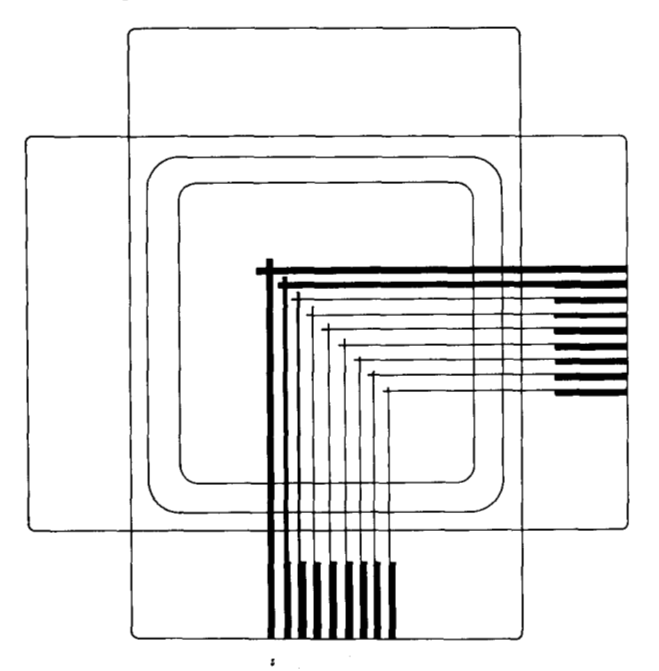
A Phenomenological Study of AC Gas Panels Fabricated with Vacuum-Deposited Dielectric Layers

Abstract: This paper presents the results of an experimental investigation of ac gas display panel parameters. The ignition and extinction voltages were measured for panels filled with Ne-0.1% Ar gas to pressures ranging from 0.75×10^4 Pa to 8×10^4 Pa (50 tort to 600 tort). The panels were constructed with chamber spacings, d, of 0.56×10^{-2} cm to 2×10^{-2} cm, and electrode widths, x, of 1.5×10^{-3} cm to 0.1 cm. Scaling of the Paschen minimum was not found to hold for the narrowest chamber spacing. The dependence of ignition voltage on linewidth was found to be proportional to exp (-1.6 x/d) for (x/d) < 1. An electron diffusion process was invoked to explain this behavior.

Introduction

The formulation of an atomic model [1] was one approach taken to better understand the operation of the ac gas display panel. The atomic model predicted dynamic write and erase voltages and static sustain voltages, as well as charge flow through the discharge and the transferred wall charge. The model did this with one adjustable parameter, the ion induced secondary emission, γ_i . How-

Figure 1 Geometry of test panel A used for linewidth and chamber spacing studies.



ever, the atomic model was limited to describing one-dimensional discharges, e.g., cells of large area. It did not account for any three-dimensional geometrical properties.

In this paper, the chamber spacing, linewidth, and pressure were systematically controlled to determine their individual effects. A qualitative explanation of some of these effects is given. With these data, proper values of minimum and maximum sustain voltages can be chosen for use in a one-dimensional model.

Experimental method

• Test panel

The panel structure used in the greater part of this study (test panel A) was fabricated by the same techniques described in the accompanying paper [2]. Chamber spacings of 0.005 cm, 0.01 cm, and 0.02 cm were employed. The electrode pattern, which is depicted in Fig. 1, consisted of nine individual cells spaced 0.36 cm from each other. The nominal linewidths were 2.5×10^{-3} , 5×10^{-3} , 1×10^{-2} , 1.5×10^{-2} , 2×10^{-2} , 2.5×10^{-2} , 5×10^{-2} , 7.6×10^{-2} , and 0.1 cm. However, the lines were up to 1×10^{-3} cm narrower due to over-etching. In all cases the exact linewidth of each cell was experimentally measured.

Other data were taken on a panel (test panel B) constructed with a 3×6 array of 18 character boxes in which the solid back lines and "tuning-fork" front lines were systematically perturbed about the mean geometry reported in the accompanying paper [2]. The geometry of the array consisted of six groups of solid back lines. The

Copyright 1978 by International Business Machines Corporation. Copying is permitted without payment of royalty provided that (1) each reproduction is done without alteration and (2) the *Journal* reference and IBM copyright notice are included on the first page. The title and abstract may be used without further permission in computer-based and other information-service systems. Permission to *republish* other excerpts should be obtained from the Editor.

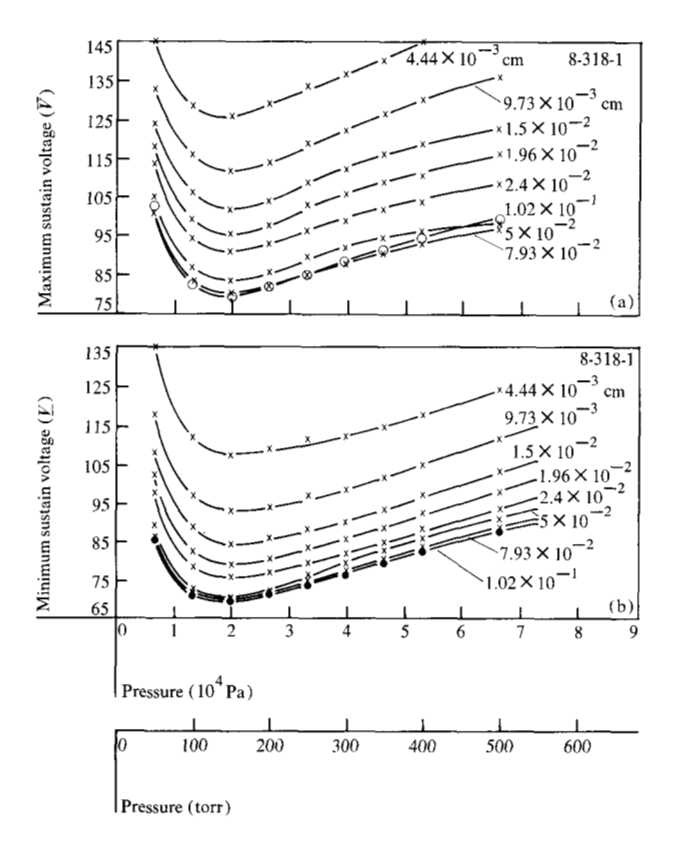


Figure 2 (a) \bar{V}_s and (b) \bar{V}_s for a Ne-0.1% Ar-filled gas panel (type A) as a function of pressure and linewidth. Chamber spacing $d = (2.06 \pm 0.07) \times 10^{-2}$ cm.

widths of the lines in the six groups varied from 2.54 \times 10^{-3} cm (1 mil) to 1.53×10^{-2} cm (6 mil), while maintaining the same 5×10^{-2} -cm (20-mil) center-to-center line spacing between each of the five back lines making up a group or character box. In a similar manner, the tuningfork front lines were generated. Three groups of seven lines each formed the front plate metallurgy. The desired tuning-fork lines consisted of two 5×10^{-3} -cm (2-mil) lines spaced 5×10^{-3} cm apart. The over-etched lines were 2.5×10^{-3} cm (1 mil) wide and spaced 7.6×10^{-3} cm (3 mil) apart, while the under-etched lines were 7.6 \times 10^{-3} cm wide and spaced 2.5×10^{-3} cm apart. This etching range constituted a ±50 percent change about the mean value. In this way conditions of over- and underetching are systematically generated. One character box had the standard or specified linewidth, while one character box had all lines etched 2.5×10^{-3} cm (1 mil) narrower than desired, and one character box had all lines etched 2.5×10^{-3} cm (1 mil) wider than desired; other combinations were also available in the matrix.

Leak-tight panels with these geometries were fabricated in the single-cycle gas panel sealing system [3] with oxide layers of $10.3 \mu m$ of borosilicate glass and $0.2 \mu m$ of MgO. For those cases where the pressure was to be varied, the "tip-off" step was omitted, and a glass-metal

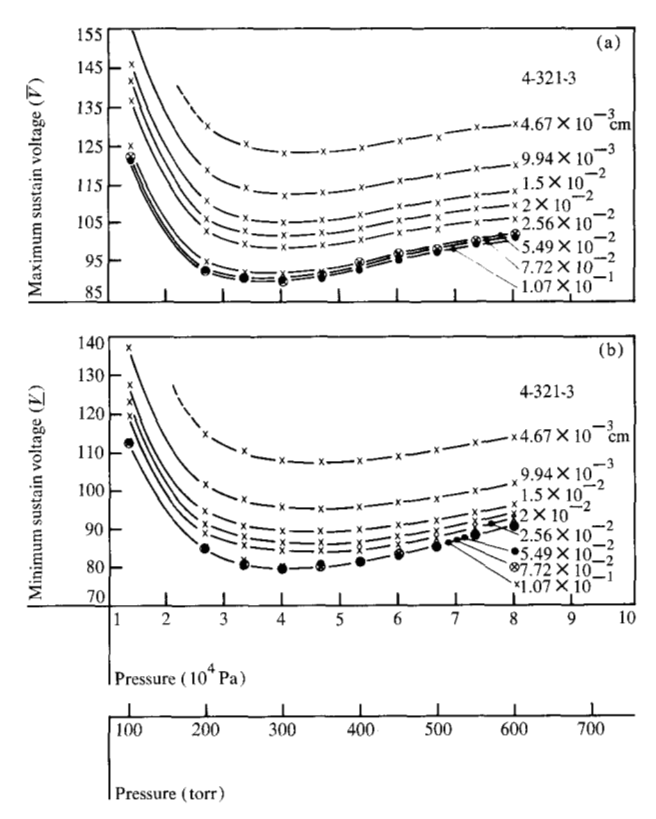


Figure 3 (a) \bar{V}_s and (b) \bar{V}_s for a Ne-0.1% Ar-filled gas panel (type A) as a function of pressure and linewidth. Chamber spacing $d = (1.07 \pm 0.07) \times 10^{-2}$ cm.

stem and a bakable high-vacuum flange were attached. The panels were then connected to a manifold where both panels and valves could be vacuum baked, after which the panels were filled with purified Ne-Ar and valved from the system. The pressure was varied from 0.75×10^4 Pa to 8×10^4 Pa (50 to 600 torr).

Measurement techniques

Test panel A, depicted in Fig. 1, was driven by a 30-kHz square wave with a rise time of 180 ns. This rise time was shorter than the avalanche formation time at all pressure-gap combinations studied. The maximum sustain (\bar{V}_s) and minimum sustain (\bar{V}_s) voltages were measured with the next larger adjacent cell in operation, except for the widest cell, in which case the next narrowest cell was in operation. Test panel B was excited by the same waveform; however, alternate lines were connected in the manner described in Fig. 2(b) of the accompanying paper [2]. In all cases the panels were operated until the voltage stabilized prior to recording data.

Results and discussion

The maximum and minimum sustain voltages (\bar{V}_s and \underline{V}_s) were measured for each cell of test panel A over the

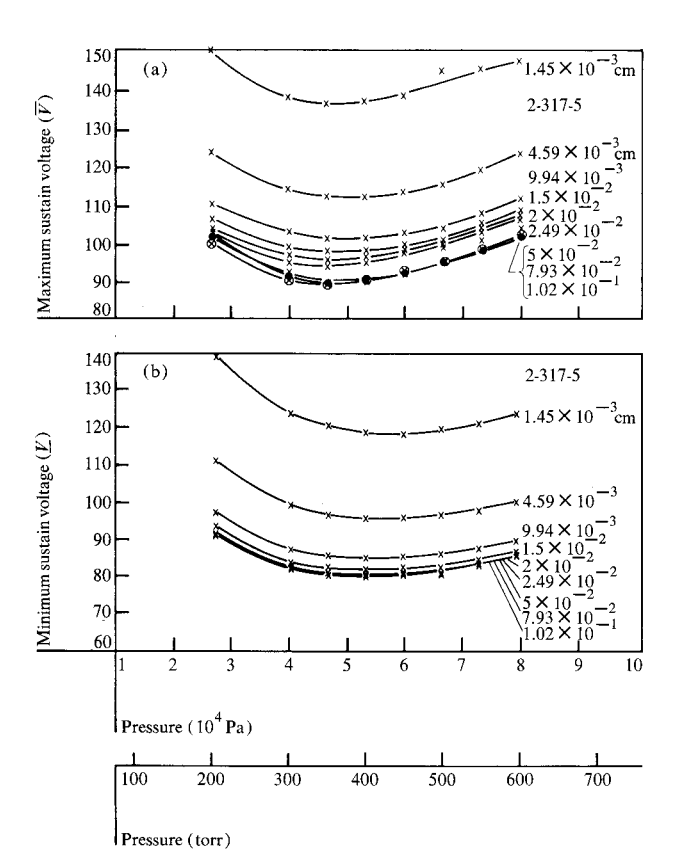


Figure 4 (a) \bar{V}_s and (b) \bar{V}_s for a Ne-0.1% Ar-filled gas panel (type A) as a function of pressure and linewidth. Chamber spacing $d=(0.56\pm0.07)\times10^{-2}$ cm.

Table 1 Pressure-spacing product for minimum ignition voltage vs panel chamber spacing.

Chamber spacing (cm)	Pd (Pa-cm)
$(2.06 \pm 0.07) \times 10^{-2}$ $(1.07 \pm 0.07) \times 10^{-2}$ $(0.56 \pm 0.07) \times 10^{-2}$	384 ± 13 392 ± 26 260 ± 33

range of chamber spacings and pressures indicated previously. Data for d=0.02 cm are given in Figs. 2(a) and (b); for d=0.01 cm in Figs. 3(a) and (b); and for d=0.0056 cm in Figs. 4(a) and (b). It was found that the classical gas filling procedure, that is, a vacuum bake prior to filling with Ne-Ar, did not produce stable operation at low voltages for panels with a chamber spacing of 0.0056 cm. As many as three sequential eight-hour vacuum bake cycles did not produce stable, low operating voltages. However, viscous cleaning, which was accomplished by successively filling and pumping between pressures of 10^4 Pa and 10^2 Pa, produced clean, stable panels. This clearly

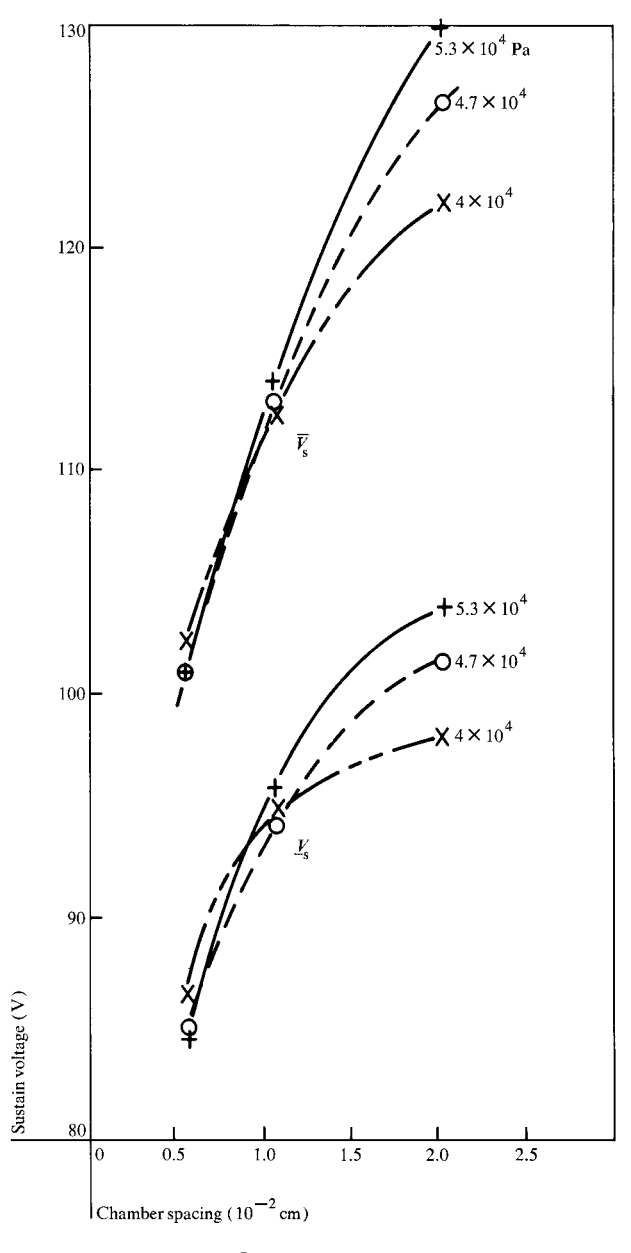


Figure 5 Variation in \bar{V}_s and \underline{V}_s with chamber spacing for a linewidth of 9.93×10^{-3} cm.

demonstrated the usefulness of employing the viscous cleaning portion of the single-cycle technique for production of panels with gas gaps less than 0.01 cm.

The experimental data presented in Figs. 2(a) and (b), 3(a) and (b), and 4(a) and (b) can be examined from two perspectives: the dependence of operating voltages on the pressure-spacing product, and on the linewidth.

• Pressure-chamber spacing effects

The "Paschen minimum," or pressure of minimum ignition voltage, was not observed to scale with the chamber spacing over the entire range (0.0056 to 0.02 cm). The

pressure-spacing products for the three spacings studied are given in Table 1. Scaling of the Paschen minimum for wide lines was observed for the 0.01- and 0.02-cm-wide spacings, but for the narrowest spacing, the pressure of minimum ignition voltage was considerably lower than expected— 5×10^4 Pa (360 torr) instead of 8×10^4 Pa (600 torr).

The Paschen minimum also varied slightly with linewidth; smaller values were observed as the linewidth of the discharge cell increased from 1.5×10^{-3} cm to 10^{-2} cm. This effect is most likely due to the slightly smaller average path length $\langle d \rangle$ for the narrower lines.

Additionally, the value of \underline{V}_s at the Paschen minimum was the same (80 V) for d=0.01 cm and 0.056 cm, while it was found to be 70 V for the 0.02-cm chamber spacing. It was to be expected that the value of \overline{V}_s would be smaller for d=0.02 cm than for d=0.01 cm, because the ionization probability exhibits a sub-linear dependence on the electric field [4]. The ionization probability for d=0.02 cm is greater than for d=0.01 cm.

It is also of interest to study the dependence of \bar{V}_s and \underline{V}_s on the chamber spacing for the case of constant pressure and constant linewidth. In Fig. 5 these data are shown for the case of 9.93 \times 10⁻³-cm-wide lines at pressures of 5.3 \times 10⁴ Pa (400 torr), 4.7 \times 10⁴ Pa (350 torr), and 4 \times 10⁴ Pa (300 torr). At a pressure of 4.7 \times 10⁴ Pa, it is necessary to hold a panel with a nominal 1 \times 10⁻²-cm chamber spacing to a tolerance of (1 \pm 0.07) \times 10⁻² cm in order that \bar{V}_s and \underline{V}_s remain within \pm 1 V of their normal values. Operating the gas panel at higher pressure places correspondingly closer tolerances on the chamber spacing. The visual appearances of discharges from 5 \times 10⁻³-cm-wide lines for the three gaps under study are illustrated in Fig. 6.

• Linewidth effects

Examination of the data in Figs. 2(a) through 4(b) shows that \bar{V}_s and \underline{V}_s increase for decreasing linewidth. In Fig. 7, \bar{V}_{s} and \bar{V}_{s} at the Paschen minimum are plotted vs linewidth. The onset of increasing \bar{V}_s , for example, was found to occur at progressively narrower linewidths as the chamber spacing was made smaller. In agreement with Hoehn and Martel [5], it was observed that wide lines more severely masked the light output. In fact, for linewidths greater than 0.025 cm, the entire area of the glow discharge cell did not spontaneously ignite. First, a corner ignited, at which point the ignition voltage was recorded, followed in succession by the second and third corner, and finally the entire cell. In some instances, initial ignition of a cell with 0.1-cm-wide lines would take the form of a small glow which would jump around the four corners in a cyclical fashion.

One must keep in mind the accuracy and repeatability of glow discharge measurements. The repeatability of any

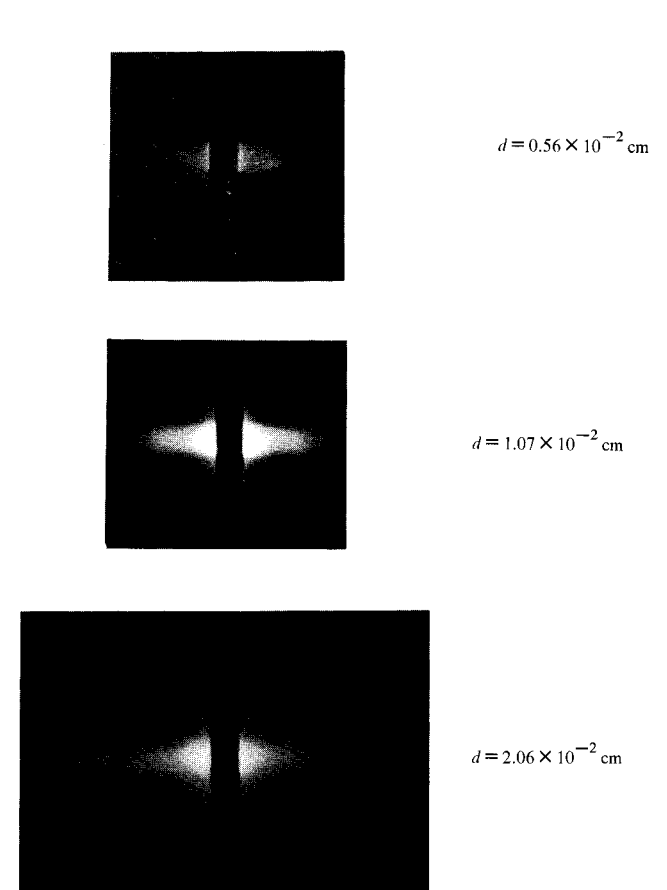


Figure 6 Spatial distribution of the glow discharge around 0.56×10^{-2} -cm-wide lines for chamber spacings of 0.56×10^{-2} cm, 1.07×10^{-2} cm, and 2.06×10^{-2} cm. The 1.07×10^{-2} -cm-wide line was exposed for twice the duration of the other two.

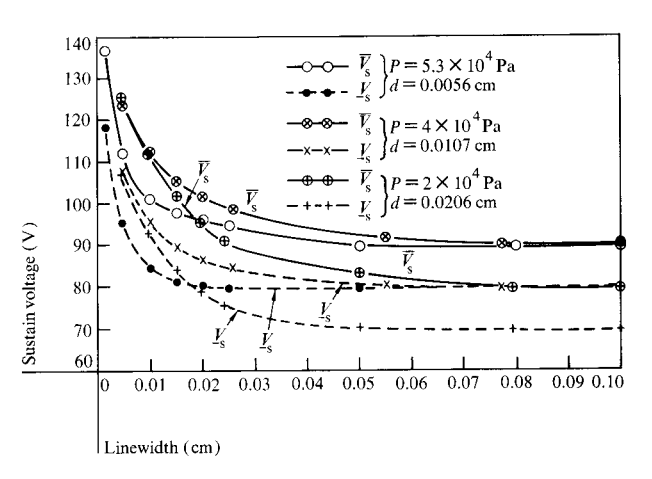


Figure 7 Variation in \bar{V}_s , V_s at the Paschen minimum for chamber spacings of 0.56×10^{-2} cm, 1.07×10^{-2} cm, and 2.06×10^{-2} cm

one measurement was within ± 0.5 V, while process control determined the device uniformity. As an example, Fig. 8 shows data taken on three identical panels for

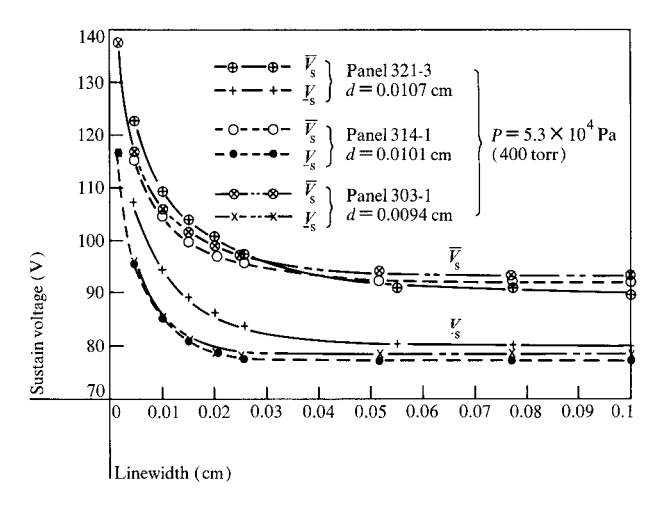


Figure 8 Variation in $\bar{V}_{\rm s}$, $\underline{V}_{\rm s}$ vs linewidth for three nominally identical panels.

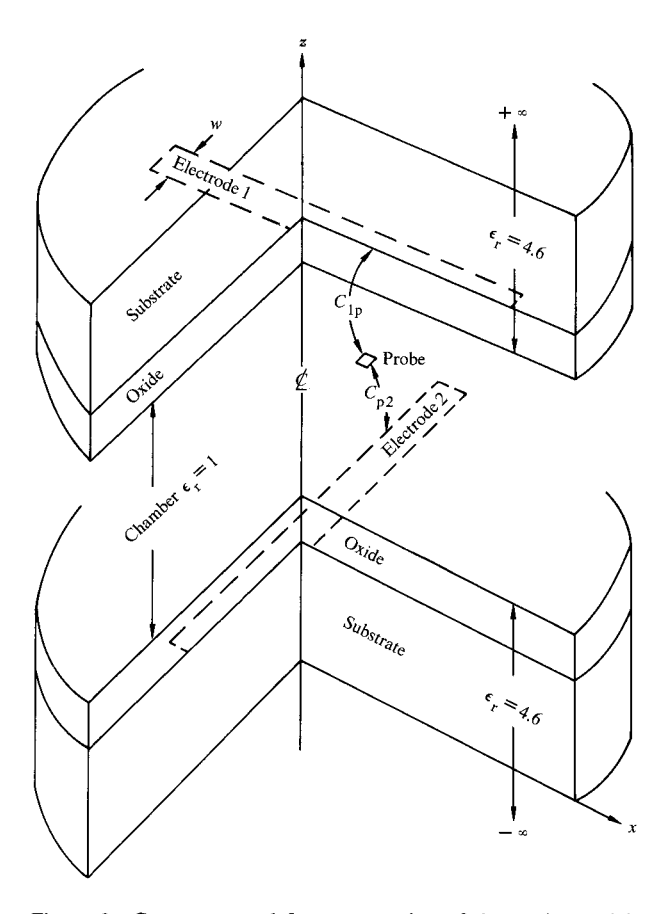


Figure 9 Geometry used for computation of the equipotentials in the chamber.

which the spread was about 4 or 5 V. All were processed in the single-cycle seal and fill system [3]. Panel 321 was removed prior to tip-off and was appended to a standard vacuum manifold in order that measurements could be

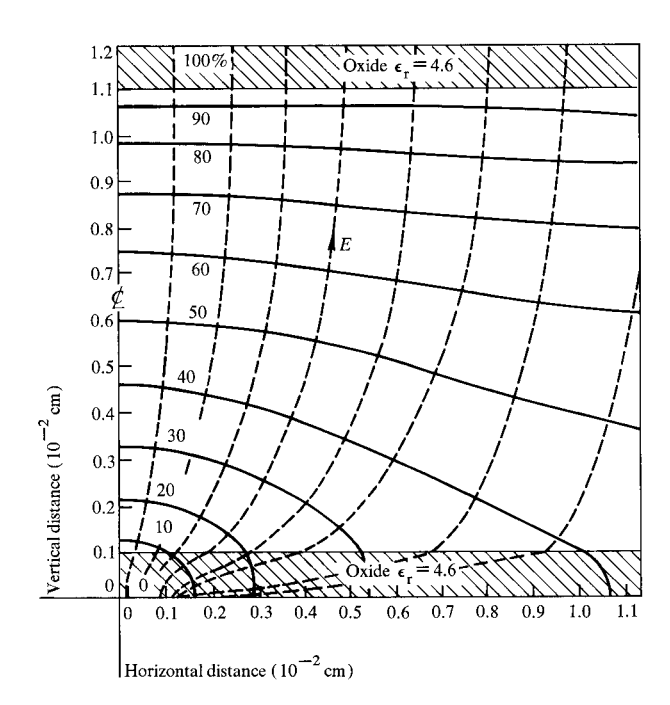


Figure 10 Equipotentials and electric field lines for lines 2.5×10^{-3} cm wide. Data are shown for the x-z positive half-plane.

made at different pressures. Panels 303 and 314 were completely processed in the single-cycle system, including filling and tip-off with 5.3×10^4 Pa (400 torr) of Ne-0.1% Ar. A spread of 2 V or less was observed between the latter two panels.

Understanding of the mechanism responsible for the variation in excitation voltage with linewidth is complicated by the geometry. The first approach was to determine the nature of electric field, E, and equipotential, V, in the region of the electrode crossing and quantitatively to observe the distortion of V and E due to the three-dimensionality of the electrodes. A computational program developed by Ruehli and Brennan [6] which was capable of calculating the node-pair capacitances for three-dimensional conductors with multilayer dielectrics was employed. The real device consisted of five dielectric layers: substrate, dielectric, gas, dielectric, and substrate. Because of limitations in the program, the substrate glass and the dielectric were considered to have the same dielectric constant (see Fig. 9). A value of $\epsilon_r = 4.6$ was measured for deposited and annealed borosilicate glass. Since the dielectric constant of the soda-lime substrate glass is 7.2, this is a good first approximation. The effect of the 0.2-\mu m-thick MgO overcoat was ignored. The program was used to compute the node-pair capacitances C_{10} and $C_{\rm p2}$ at 10^{-3} -cm intervals in the positive x-z half-plane. The probe was a mathematical electrode 2.5×10^{-4} cm square with zero thickness. In those instances where the equipotentials were in the direction of the z axis, the probe was

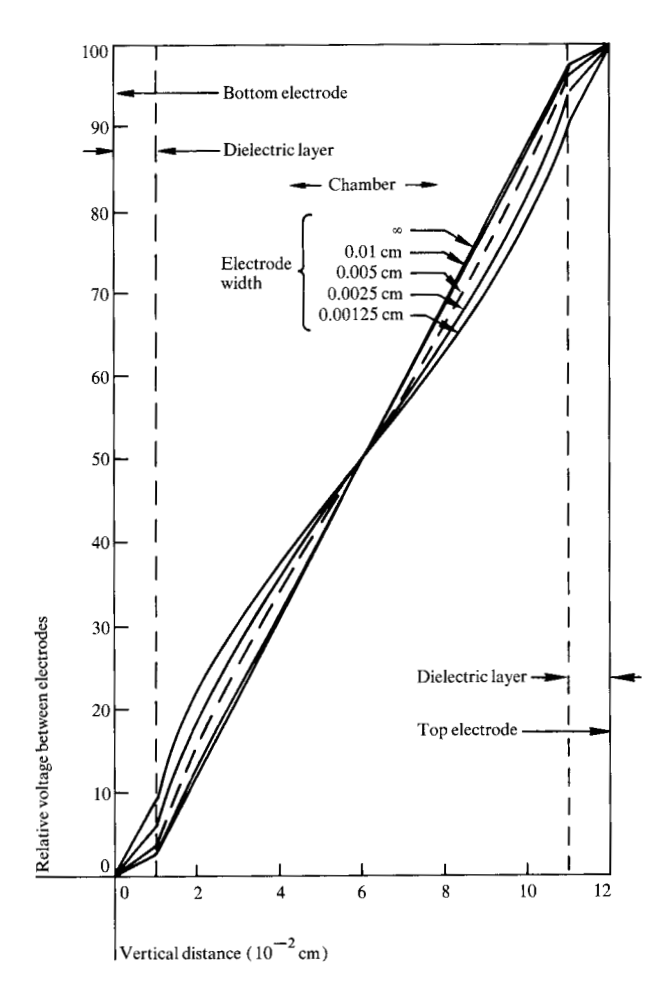


Figure 11 Calculated potential distribution along the z axis at y = x = 0 as a function of linewidth.

rotated accordingly. From these data the relative equipotentials were calculated for two cells with d=0.01 cm, line lengths of 0.05 cm, dielectric layers of $\epsilon_{\rm r}=4.6$, and thicknesses of 0.001 cm. Figure 10 displays the resulting equipotentials and fields for zero thickness electrodes of width x=0.0025 cm. Examination of Fig. 10 reveals that the equipotentials were considerably different than would be obtained for the case of infinitely wide or two-dimensional electrodes.

In Fig. 11 the potential along the z axis (x = y = 0) is plotted for four different linewidths, $x = \infty$, 0.01, 0.005, 0.0025, and 0.0125 cm. These data were calculated for the chamber spacing and dielectric parameters previously specified. From this it was seen that the changes in average electric field for linewidths between 0.01 cm and ∞ were insignificant in the center of the active region, while the maximum sustain or the ignition voltage of an isolated cell increased 15 to 20 percent in the region x = 0.01 to 0.1 cm. Thus, the increased ignition voltage observed for narrow linewidths cannot be due singly to the reduction in

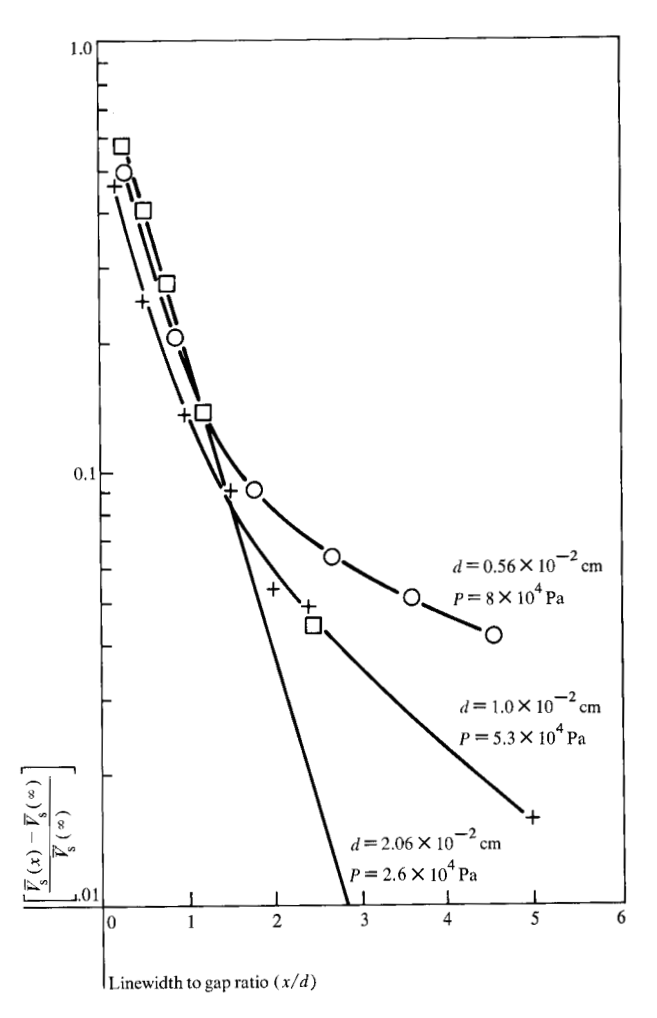


Figure 12 Fractional increase in ignition voltage as a function of the linewidth-to-chamber spacing ratio for the three chamber spacings fabricated.

the peak electric field in the central region of the glow brought about by the more point-like nature of the electrodes. In fact, in the region near the dielectric surfaces, narrow electrodes produce higher electric fields than do wide electrodes for the same applied potential.

A phenomenon that can account for the magnitude of increased ignition potential of narrow lines is significant lateral diffusion of hot electrons into the surrounding gas space. Hot electrons are scattered into the adjacent regions of the lower field where the probability of ionization is less; increasing the applied potential increases the volume of gas in which the electric field is high enough to produce an avalanche, before the electrons diffuse into the surrounding gas.

In Fig. 12 the fractional increase in operating voltage has been plotted as a function of a linewidth-to-chamber spacing ratio, x/d, for the three spacings previously studied. In all cases scaling was observed only in the region $(x/d) \le 1$. In this region the diffusion loss of hot electrons

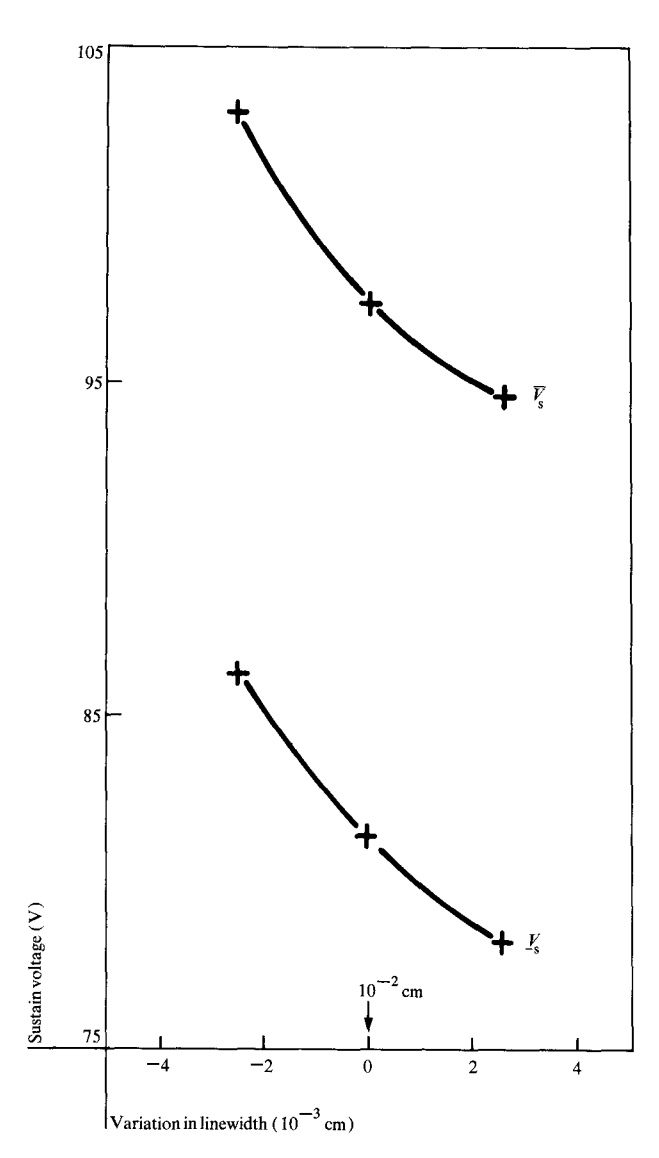


Figure 13 Variation in \tilde{V}_s , V_s with linewidth for $d=10^{-2}$ cm, $P=5.3\times10^4$ Pa using the electrode geometry of test panel B.

to the surrounding region dominates over drift to the dielectric surface. It was observed that the dependence of voltage on linewidth was proportional to

$$\frac{\bar{V}_{\rm s}(x) - \bar{V}_{\rm s}~(\infty)}{\bar{V}_{\rm s}~(\infty)} \propto \exp{(-1.6~x/d)}.$$

For the region (x/d)>1, the region where surface losses dominated, similarity was not observed. It was also noted that data in the region $\bar{V}(x)-\bar{V}$ $(\infty)\leq 0.05\ \bar{V}$ (∞) were subject to errors in measurement because the entire cell was not ignited spontaneously, as well as the usual errors incurred when taking a small difference between two large numbers. Although there are differences in voltages for panels with the same large x/d, but different d, the data are not accurate enough for analysis.

• Margin loss due to linewidth variations

The observation that linewidth variations caused changes in the sustain voltages portended problems unless close tolerances were held in the manufacture of the metal lines. Over-etching or a local narrow spot on a line due to a photoresist defect caused the minimum sustain to locally increase, and under-etching or a local wide spot due to splatter from the metal deposition source caused the maximum sustain to locally decrease. Either of these caused the effective or overall panel memory margin to decrease. The worst case for an individual cell was the concurrence of two such spots.

Although the data were available from the geometry of test panel A, a second geometry, test panel B, was used to simulate a more realistic condition—that of split or tuning-fork front lines arranged in arrays of character boxes that could be subjected to the static test. Test panel B was fabricated to obtain this quantitative data. Figure 13 illustrates the observed behavior of the sustain voltages with test panel B using the static test, that is, with alternate lines excited in each character box. The worst loss, the concurrence of a wide and a narrow line, resulted in the greatest loss of memory margin, which was found to be $-1.5 \text{ V per } 10^{-3} \text{ cm}$ of linewidth. Two thirds of the measured loss was attributed to the front lines. To keep the memory margin loss to 2 V, it was necessary to hold the linewidth to within $\pm 1.33 \times 10^{-3}$ cm of the dimensions specified for these lines.

Conclusion

Several facets of gas display panel operation were made apparent in this study. The scaling of the Paschen minimum was not observed to hold for the narrowest chamber spacing considered (0.56 \times 10⁻² cm). Additionally, a slight sensitivity of the Paschen minimum to linewidth was observed in all cases. For lines of width 0.01 cm, the variation in \bar{V}_s with chamber spacing was found to be 7×10^{-4} cm/volt at a pressure of 4.7×10^{-4} Pa.

The large changes in ignition voltage with linewidth could not be attributed to the changes in either peak electric field or average electric field in the center of the cell area. One reasonable explanation is the lateral diffusion of hot electrons into the surrounding gas. This is consistent with data showing the dependence of the fractional increase in ignition voltage to have the same dependence on (x/d) where (x/d) < 1. In that region the surrounding gas accounts for most of the surface area of the active region.

For devices with tuning-fork front electrodes, it was observed that the loss of memory margin with linewidth variation was $-1.5 \text{ V}/10^{-3} \text{ cm}$. Two thirds of this loss was found to be associated with the front plate tuning-fork electrode because over-etching the tuning-fork removes two times as much metal as over-etching a single line.

Although the front electrode is better optically, it does require closer tolerances in manufacture to hold down operating voltage variations caused by improper etching of the metallurgy.

References

- 1. C. Lanza and O. Sahni, IBM J. Res. Develop. 22, 641 (1978, this issue).
- John F. O'Hanlon, K. C. Park, A. Reisman, R. Havreluk, and J. G. Cahill, IBM J. Res. Develop. 22, 613 (1978, this issue).
- 3. A. Reisman, M. Berkenblit, and S. A. Chan, IBM J. Res. Develop. 22, 596 (1978, this issue).
- A. A. Kruithof and F. M. Penning, *Physica Lett.* 4, 430 (1936).

- H. J. Hoehn and R. A. Martel, IEEE Trans. Electron Devices ED-18, 659 (1971).
- A. E. Ruehli and P. A. Brennan, IEEE J. Solid-State Circuits SC-10, 530 (1975).

Received September 29, 1977; revised November 14, 1977

The author is located at the IBM Thomas J. Watson Research Center, Yorktown Heights, New York 10598.